Journal of Applied Analysis and Computation
Volume 15, Number 6, December 2025, 3207–3225
Website:http://www.jaac-online.com
DOI:10.11948/20250018

NUMERICAL SOLUTION OF FRACTIONAL SINGULAR PERTURBATION CAUCHY PROBLEM*

Guocai Cai[1] and Qingxia Liu[1,2,†]

Abstract In this work, we consider a singularly perturbed Cauchy problem where the small parameter ε appears in the highest-order derivative term (i.e., the fractional derivative). First, we analyze some properties of the fractional singular perturbation problem. Then, a Shishkin mesh is introduced to address it, as traditional numerical methods for singularly perturbed problems may lead to numerical instability. Finally, we present numerical results demonstrating good stability and accuracy.

Keywords Fractional singular perturbation, numerical solution, Shishkin meshes.

MSC(2010) 34A08, 34E15, 65Lxx.

1. Preliminary

The singular perturbation problem arises in many fields such as fluid mechanics, elastic mechanics, quantum mechanics, acoustics, optics, chemical reactions, and optimal control. Its characteristic is that the differential equation contains a perturbation parameter, which can either naturally occur reflecting certain physical properties or be artificially introduced. Generally their exact solutions can not be obtained easily. Then it turns to numerical methods for assistance, which is more efficient than asymptotical method due to the highly developed computing technology nowadays.

The research of asymptotical method for the traditional singular perturbation problem with integer order derivative has been an active branch in applied mathematics already [3–5, 12, 17]. A large number of literatures have emerged about research work for asymptotical solution of singular perturbation. The research referring to numerical method for singular perturbation appears relatively late. The reason is that the numerical solution of such problems is quite difficult. For example, for boundary layer singular perturbation problem, the small parameter ε

†The corresponding author.
1School of Mathematical Sciences, Xiamen University, Xiamen, China
2Fujian Provincial Key Laboratory of Mathematical Modeling and High-Performance Scientific Computing, Xiamen University, Xiamen, Fujian, China
*The authors were supported by the Natural Science Foundation of Fujian Province of China (Grant Nos. 2022J01035 and 2023J01026) and the National Natural Science Foundation of China (Grant Nos. 12371372, 12371081 and 12271450).
Email: gotry@xmu.eud.cn(G. Cai), liuqx@xmu.edu.cn(Q. Liu)

exists in the highest order derivative term of the differential equation, this leads to the differential equation's order will reduce, then its definite solution conditions will lose partly or totally, when the small parameter $\varepsilon = 0$. Since it is the function of the small parameter ε, the solution's great changes have taken place near the boundary where lose the definite solution condition, which is called boundary layer singularity.

The same difficulty exists in the fractional order singular perturbation problems. There were some references on the research of singular perturbation problem with fractional derivative already [1, 2, 7–9, 15, 16, 18, 20, 22]. However, most of them involved in numerical method focused on asymptotical method [2,7,9,18,20]. Some involved in numerical solution were considered with $\alpha(1 < \alpha < 2)$ fractional order derivative [1, 22], [15]. Several literatures [15] focused on one with $\alpha(0 < \alpha < 1)$ Caputo fractional order derivative. Mostafa et al. [15] consider singular perturbation problem with the Caputo-Fabrizio derivative and propose a special solution using the Laplace iterative methods.

We consider in this work the following singular perturbation problem with fractional derivative:

$$\begin{cases} L_\varepsilon \equiv \varepsilon^\alpha \, {}_0^{\mathrm{C}}D_x^\alpha u(x) + a(x)u(x) = f(x), \;\; x \in [0, L], \\ u(0) = \phi \end{cases} \tag{1.1}$$

where $0 < \alpha \leq 1$, $a(x) \geq \beta > 0$ and the Caputo fractional derivative ${}_0^{\mathrm{C}}D_x^\alpha$ is defined by [14]:

$${}_0^{\mathrm{C}}D_x^\alpha v(x) = \frac{1}{\Gamma(1-\alpha)} \int_0^x \frac{v'(\tau)}{(x-\tau)^\alpha} d\tau,$$

and in this paper ${}_0^{\mathrm{C}}D_x^{n\alpha}$ means $\underbrace{{}_0^{\mathrm{C}}D_x^\alpha {}_0^{\mathrm{C}}D_x^\alpha \cdots {}_0^{\mathrm{C}}D_x^\alpha}_{\text{n-times}}$.

The properties of the Caputo fractional derivative are listed in the following, which are referred to in the section of numerical experiment.

Lemma 1.1. ${}_0^{\mathrm{C}}D_x^\alpha f(kx) = k {}_0^{\mathrm{C}}D_x^\alpha f(x)$.

One-variable Mittag-Leffler function is defined by [6]:

$$E_\alpha(z) = \sum_{k=0}^{+\infty} \frac{z^k}{\Gamma(1+k\alpha)}, \quad \alpha > 0, \; |z| < \infty.$$

Lemma 1.2. *The Caputo derivative of the Mittag-Leffler function satisfies the following linear property:*

$${}_0^{\mathrm{C}}D_x^\alpha E_\alpha(-\lambda x^\alpha) = -\lambda E_\alpha(-\lambda x^\alpha). \tag{1.2}$$

Proof.

$$\begin{aligned} {}_0^{\mathrm{C}}D_x^\alpha E_\alpha(-\lambda x^\alpha) &= {}_0^{\mathrm{C}}D_x^\alpha \sum_{k=1}^{\infty} \frac{(-\lambda x^\alpha)^k}{\Gamma(k\alpha+1)} \\ &= \sum_{k=1}^{\infty} \frac{(-\lambda)^k {}_0^{\mathrm{C}}D_x^\alpha x^{k\alpha}}{\Gamma(k\alpha+1)} \end{aligned}$$

$$= \sum_{k=1}^{\infty}(-\lambda)^k \frac{\Gamma(k\alpha+1)x^{(k\alpha+1-\alpha)}}{\Gamma(k\alpha-\alpha)\Gamma(k\alpha+1)}$$
$$= -\lambda \sum_{k=0}^{\infty} \frac{(-\lambda x^{\alpha})^k}{\Gamma(k\alpha+1)}$$
$$= -\lambda E_{\alpha}(-\lambda x^{\alpha}).$$

due to the formula ${}_0^{\mathrm{C}}D_x^{\alpha}C = 0$ (C is a const) and ${}_0^{\mathrm{C}}D_x^{\alpha}x^{\gamma} = \frac{\Gamma(\gamma+1)}{\Gamma(\gamma-\alpha+1)}x^{\gamma-\alpha}$ $(\gamma > \alpha)$. □

2. Properties of fractional singular perturbation Cauchy problem's solution

To deduce the properties of the solution for the singular perturbation problem (1.1), introduce the Maximum theorem of the fractional derivative.

Lemma 2.1 (Maximum theorem). [11] *For* $f \in C^1(0,X) \cap C[0,X]$, $f(x_0) = \min\limits_{x\in[0,X]} f(x)$, $0 < \alpha < 1$, *then* ${}_0^{C}D_{x_0}^{\alpha} f(x_0) \le 0$.

Utilizing the Maximum theorem, the following lemmas are obtained.

Lemma 2.2. *Suppose*

- *(i)* v *is a smooth function;*
- *(ii)* $v(0) \ge 0, X > 0$*;*
- *(iii)* $L_{\varepsilon}v(x) \ge 0$ *for* $x \in [0,X]$,

then it holds $v(x) \ge 0, \forall x \in [0,X]$.

Proof. Proof by contradiction is considered in the following. Denote that

$$v(x_0) = \min_{x\in[0,X]} v(x),$$

suppose that

$$v(x_0) < 0,$$

then

$${}_0^{C}D_{x_0}^{\alpha} v(x_0) \le 0$$

due to Lemma 2.1, it is contrast to

$$L_{\varepsilon}v(x) \equiv \varepsilon^{\alpha}{}_0^{\mathrm{C}}D_x^{\alpha}v + a(x)v(x) \ge 0,$$

then $v(x) \ge 0$. □

Lemma 2.3 (Stability inequality). *Suppose*

- *(i)* v *is a smooth function;*
- *(ii)* $X > 0$*;*

then $|v(x)| \le |v(0)| + \frac{1}{\beta}\max\limits_{0\le y\le x}|L_{\varepsilon}v(y)|$, $a(x) \ge \beta > 0$.

Proof. Construct two functions

$$w_+(x) = |v(0)| + \frac{1}{\beta}\max_{0\le y\le x}|L_\varepsilon v(y)| + v(x),$$
$$w_-(x) = |v(0)| + \frac{1}{\beta}\max_{0\le y\le x}|L_\varepsilon v(y)| - v(x),$$

it is clear $w_+(x) \ge 0,\ w_-(x) \ge 0$. Then it has

$$L_\varepsilon w_\pm(x) = a(x)|v(0)| + \frac{a(x)}{\beta}\max_{0\le y\le x}|L_\varepsilon v(y)| \pm L_\varepsilon v(x) \ge 0.$$

From Lemma 2.2, it obtains $w_\pm(x) \ge 0,\ x \in [0, X]$. □

In the following we prove the solution fulfils the property when the coefficient $a(x)$ is a constant.

Theorem 2.1. *Suppose*

- *(i)* $X > 0$*;*
- *(ii)* $L_\varepsilon \equiv \varepsilon^\alpha {}_0^{\mathrm{C}}D_x^\alpha + a$*;*

then for any $v(x)$ *which fulfils*

$$\left|{}_0^{\mathrm{C}}D_x^{n\alpha} L_\varepsilon v(x)\right| \le C,\ \textit{for}\ n \ge 0,\ 0 < x < X,$$

the following estimate holds

$$\left|{}_0^{\mathrm{C}}D_x^{n\alpha} v(x)\right| \le C\varepsilon^{-n\alpha},\ n \ge 0,\ 0 < x < X.$$

If $av(0) = L_\varepsilon v(0)$*,then*

$$\left|{}_0^{\mathrm{C}}D_x^{n\alpha} v(x)\right| \le C(2 + \varepsilon^{(1-n)\alpha}),\ n \ge 0,\ 0 < x < X,$$

where C *is independence to* ε*.*

Proof. Due to $L_\varepsilon v(x) = \varepsilon^\alpha {}_0^{\mathrm{C}}D_x^\alpha v + av$, we get

$${}_0^{\mathrm{C}}D_x^\alpha v = \frac{1}{\varepsilon^\alpha}[L_\varepsilon v(x) - av(x)],$$

based on the assumption, it obtains

$$\left|{}_0^{\mathrm{C}}D_x^\alpha v(x)\right| \le C\varepsilon^{-\alpha},$$

and

$$\begin{aligned}
\left|{}_0^{\mathrm{C}}D_x^{2\alpha} v(x)\right| &= \frac{1}{\varepsilon^\alpha}\left|{}_0^{\mathrm{C}}D_x^\alpha[L_\varepsilon v - av]\right| \\
&= \frac{1}{\varepsilon^\alpha}\left|{}_0^{\mathrm{C}}D_x^\alpha L_\varepsilon v - a{}_0^{\mathrm{C}}D_x^\alpha v\right| \\
&= \frac{1}{\varepsilon^\alpha}\left|{}_0^{\mathrm{C}}D_x^\alpha L_\varepsilon v - a\frac{1}{\varepsilon^\alpha}[L_\varepsilon v(x) - av(x)]\right| \\
&\le C\varepsilon^{-2\alpha},
\end{aligned}$$

due to Lemma 1.1.

We then have by the Mathematical induction that

$$\left|{}_0^{\mathrm{C}}D_x^{n\alpha}v(x)\right| = \frac{1}{\varepsilon^\alpha}\left|{}_0^{\mathrm{C}}D_x^{(n-1)\alpha}(L_\varepsilon v(x) - av(x))\right|.$$

If $\left|{}_0^{\mathrm{C}}D_x^{(n-1)\alpha}v(x)\right| \le C\varepsilon^{-(n-1)\alpha}$, then

$$\left|{}_0^{\mathrm{C}}D_x^{n\alpha}v(x)\right| \le C\varepsilon^{-n\alpha}.$$

So far, we arrive the first part of the conclusion.

Since $L_\varepsilon v = \varepsilon^\alpha {}_0^{\mathrm{C}}D_x^\alpha + av$, it holds

$$v(x) = \frac{1}{a}[L_\varepsilon v(x) - \varepsilon^\alpha {}_0^{\mathrm{C}}D_x^\alpha v(x)].$$

Let $z(x) = -\frac{1}{a}{}_0^{\mathrm{C}}D_x^\alpha v(x)$, then

$$v(x) = \frac{1}{a}L_\varepsilon v(x) + \varepsilon^\alpha z(x),$$

then the function $z(x)$ fulfils

$$\begin{cases} L_\varepsilon z(x) = -\dfrac{1}{a}L_\varepsilon v(x), \\ z(0) = 0. \end{cases}$$

In fact,

$$z(x) = \frac{1}{\varepsilon^\alpha}[v(x) - \frac{1}{a}L_\varepsilon v(x)],$$

and

$$L_\varepsilon z(x) = \frac{1}{\varepsilon^\alpha}[L_\varepsilon v(x) - (\varepsilon^\alpha \frac{1}{a}{}_0^{\mathrm{C}}D_x^\alpha L_\varepsilon v(x) + a\frac{1}{a}L_\varepsilon v(x))] = -\frac{1}{a}L_\varepsilon v(x),$$

and the initial condition can be acquired from $v(0) = \frac{1}{a}L_\varepsilon v(0) + \varepsilon^\alpha z(0)$, it leads $z(0) = 0$ under the condition $av(0) = L_\varepsilon v(0)$.

Applying the first part of the conclusions to $z(x)$, it leads to

$$\left|{}_0^{\mathrm{C}}D_x^{n\alpha}z(x)\right| \le C\varepsilon^{-n\alpha}.$$

Again from

$$v(x) = \frac{1}{a}L_\varepsilon v(x) + \varepsilon^\alpha z(x),$$

it arrives

$$\left|{}_0^{\mathrm{C}}D_x^{n\alpha}v(x)\right| \le \left|\frac{1}{a}{}_0^{\mathrm{C}}D_x^{n\alpha}v(x)\right| + \varepsilon^\alpha\left|{}_0^{\mathrm{C}}D_x^{n\alpha}z(x)\right| \le C(1+\varepsilon^{-(1-n)\alpha}).$$

$\square$

3. Numerical solution

3.1. Difference scheme with uniform mesh nodes

Discretize the Caputo fractional derivative as the following form [21]:

$$ {}_0^C D_{x,h}^{\alpha} f(x_k) = \frac{h^{-\alpha}}{\Gamma(2-\alpha)} \sum_{j=0}^{k} b_j^{(1-\alpha)} [f(x_{k+1-j}) - f(x_{k-j})], \tag{3.1} $$

where

$$ b_j^{(\alpha)} = (j+1)^{\alpha} - j^{\alpha}. \tag{3.2} $$

And

$$ {}_0^{\mathrm{C}} D_x^{\alpha} f(x_k) = {}_0^C D_{x,h}^{\alpha} f(x_k) + R_k \tag{3.3} $$

where

$$ |R_k| \le C\tau^{2-\alpha}. $$

Then we give the difference scheme for the problem (1.1):

$$ \begin{cases} \varepsilon^{\alpha} \sum\limits_{j=0}^{k} b_j^{(1-\alpha)} [u_{k+1-j} - u_{k-j}] + \nu a_{k+1} u_{k+1} = \nu f_{k+1}, \\ u_0 = \phi \end{cases} $$

which can be rewritten as

$$ \begin{cases} (\varepsilon^{\alpha} b_0^{(1-\alpha)} + \nu a_{k+1}) u_{k+1} = \nu f_{k+1} + b_0 u_k + \sum\limits_{j=0}^{k-1} b_{k-j}^{(1-\alpha)} (u_{j+1} - u_j), \\ u_0 = \phi \end{cases} \tag{3.4} $$

for $k = 1, 2, \cdots, N$ and $\nu = h^{\alpha}\Gamma(2-\alpha)$.

Since the change of the solution is minimal outside the boundary layer, numerical simulations on uniform grids result in excessive computational costs. We refer to the treat of the traditional singular perturbation problem with integer order. Numerical approximation with Shishkin mesh nodes can reduce the calculation cost while maintain the accuracy [12].

3.2. Difference scheme with Shishkin mesh nodes

Let N be a positive even number and take the breaking point σ as

$$ \sigma = \min\{\frac{1}{2}, \frac{2\varepsilon}{c} \ln(N)\}, $$

which is selected as experiment parameter in singular perturbation problem [12, 13, 19].

In this section we take

$$ \sigma = 2\varepsilon \ln(N). $$

Then equally devide the intervals $[0, \sigma]$ and $[\sigma, T]$ as follows:

$$ x_k = \begin{cases} \dfrac{2\sigma}{N} k, & 0 \le k \le \dfrac{N}{2}, \\ \sigma + \dfrac{2(1-\sigma}{N} \left(k - \dfrac{N}{2}\right), & \dfrac{N}{2} < k \le N, \end{cases} $$

and mesh step $h_k = x_k - x_{k-1}$ satisfies

$$h_k = \begin{cases} h_1 = \dfrac{2\sigma}{N}, & 0 \le k \le \dfrac{N}{2}, \\ h_2 = \dfrac{2(1-\sigma)}{N}, & \dfrac{N}{2} < k \le N. \end{cases}$$

Next, we construct the numerical discretization for the Caputo derivative at the nodes which cross the breaking point σ, i.e. $k > \frac{N}{2}$,

$$\begin{aligned}
&{}_0^C D_{x,h}^{\alpha} f(x_k) \\
=&\frac{1}{\Gamma(1-\alpha)} \int_0^{x_{k+1}} \frac{f'(\tau)}{(x_{k+1}-\tau)^{\alpha}} d\tau \\
=&\frac{1}{\Gamma(1-\alpha)} \sum_{j=0}^{k} \int_{x_j}^{x_{j+1}} \frac{f'(\tau)}{(x_{k+1}-\tau)^{\alpha}} d\tau \\
=&\frac{1}{\Gamma(2-\alpha)} \sum_{j=0}^{\frac{N}{2}-1} \frac{f_{j+1}-f_j}{h_1} [(x_{k+1}-x_j)^{1-\alpha} - (x_{k+1}-x_{j+1})^{1-\alpha}] \\
&+ \frac{1}{\Gamma(2-\alpha)} \sum_{j=\frac{N}{2}}^{k} b_{k-j}^{(1-\alpha)} \frac{f_{j+1}-f_j}{h_2^{\alpha}}.
\end{aligned}$$

Denote $\nu_1 = h_1^{\alpha}\Gamma(2-\alpha), \nu_2 = h_2^{\alpha}\Gamma(2-\alpha), \nu_{21} = h_2^{\alpha}/h_1$, the numerical scheme with Shishkin mesh nodes is constructed as:

$$\begin{cases}
\varepsilon^{\alpha} \displaystyle\sum_{j=0}^{k} b_j^{(1-\alpha)} [u_{k+1-j} - u_{k-j}] + \nu_1 a_{k+1} u_{k+1} = \nu_1 f_k, & 0 \le k \le \dfrac{N}{2}, \\
\varepsilon^{\alpha} (\nu_{21} \displaystyle\sum_{j=0}^{\frac{N}{2}-1} [(x_{k+1}-x_j)^{1-\alpha} - (x_{k+1}-x_{j+1})^{1-\alpha}][u_{k+1-j} - u_{k-j}] & \\
+ \displaystyle\sum_{j=\frac{N}{2}}^{k} b_j^{(1-\alpha)} [u_{k+1-j} - u_{k-j}]) + \nu_2 a_{k+1} u_{k+1} = \nu_2 f_k, & \dfrac{N}{2} < k \le N, \\
u_0 = \phi, &
\end{cases} \tag{3.5}$$

which can be written as:

for $0 \le k \le \frac{N}{2}$,

$$(\varepsilon^{\alpha} b_0^{(1-\alpha)} + \nu_1 a_{k+1}) u_{k+1} = \nu_1 f_k + \varepsilon^{\alpha} \{ b_0^{(1-\alpha)} u_k - \sum_{j=0}^{k-1} b_j^{(1-\alpha)} [u_{k+1-j} - u_{k-j}] \},$$

for $\frac{N}{2} < k \le N$,

$$\begin{aligned}
&(\varepsilon^{\alpha} b_0^{(1-\alpha)} + \nu_2 a_{k+1}) u_{k+1} \\
=&\nu_2 f_k + \varepsilon^{\alpha} \{ b_0^{(1-\alpha)} u_k - \sum_{j=\frac{N}{2}}^{k-1} b_j^{(1-\alpha)} [u_{k+1-j} - u_{k-j}]
\end{aligned}$$

$$+\nu_{21}\sum_{j=0}^{\frac{N}{2}-1}[(x_{k+1}-x_j)^{1-\alpha}-(x_{k+1}-x_{j+1})^{1-\alpha}][u_{k+1-j}-u_{k-j}]\}.$$

3.3. Stability analysis

Lemma 3.1 (Discrete Maximum theorem)**.** *For a mesh function* f_i $(i=0,1,\cdots)$, *suppose* $f_{i_0}=\min\{f_i\}$, $0<\alpha<1$, *then* ${}_0^C D_{x,h}^{\alpha} f(x_{i_0})\leq 0$.

Proof. Rewrite the discretization of the Caputo fractional derivative (3.1) as

$${}_0^C D_{x,h}^{\alpha} f(x_k)=\frac{h^{-\alpha}}{\Gamma(2-\alpha)}[b_0^{(1-\alpha)}f_k-b_{k-1}^{(1-\alpha)}f_0-\sum_{j=1}^{k-1}(b_{j-1}^{(1-\alpha)}-b_j^{(1-\alpha)})f(x_{k-j})].$$

Due to $f_{i_0}=\min\{f_i\}$, it obtains

$$\begin{aligned}{}_0^C D_{x,h}^{\alpha} f_{i_0}&=\frac{h^{-\alpha}}{\Gamma(2-\alpha)}[b_0^{(1-\alpha)}f_{i_0}-b_{i_0-1}^{(1-\alpha)}f_0-\sum_{j=1}^{i_0-1}(b_{j-1}^{(1-\alpha)}-b_j^{(1-\alpha)})f_{i_0-j}]\\&\leq\frac{h^{-\alpha}}{\Gamma(2-\alpha)}[b_0^{(1-\alpha)}-b_{i_0-1}^{(1-\alpha)}-\sum_{j=1}^{i_0-1}(b_{j-1}^{(1-\alpha)}-b_j^{(1-\alpha)})]f_{i_0}\\&=0\end{aligned}$$

since $-f_j\leq -f_{i_0}$ and $b_j^{(1-\alpha)}>0$, $b_{j-1}^{(1-\alpha)}-b_j^{(1-\alpha)}>0$ for $j=0,1,\cdots$.

Similar to Lemmas 2.2 and 2.3, the following lemmas, and stability inequality are obtained. □

Lemma 3.2. *Suppose*

- *(i)* v_i $(i=0,1,2,\cdots)$ *is a mesh function;*
- *(ii)* $v_0\geq 0$*;*
- *(iii)* $L_\varepsilon^h v_i=\varepsilon^{\alpha}{}_0^C D_{x,h}^{\alpha}v_i+a_iv_i\geq 0,\ i=1,2,\cdots,$

then it holds $v_i\geq 0,\forall i=1,2,\cdots$.

Lemma 3.3. *Suppose that* v_i $(i=0,1,2,\cdots)$ *is a mesh function, and* $X>0$, *then it holds* $|v_i|\leq|v(0)|+\frac{1}{\beta}max|L_\varepsilon^h v_j|,\ a_i\geq\beta>0$.

Therefore, we have the following Discrete Stability inequality due to the above lemmas.

Theorem 3.1 (Discrete Stability inequality)**.** *The solution of difference equations* u_i^h *satisfies*

$$\left|u_i^h\right|\leq|\phi|+\frac{1}{\beta}\max_{0\leq ih\leq X}|f(x_j)|.$$

4. Numerical experiments

4.1. An example with homogeneous term

In this section we first consider the following homogeneous problem:

$$\begin{cases} \varepsilon^{\alpha}\,{}_{0}^{\mathrm{C}}D_{x}^{\alpha}u(x)+u(x)=0, \quad x\in(0,1], \\ u(0)=1, \end{cases}$$

where $\alpha = 0.95$ and the exact solution is $u(x) = E_{\alpha}(-\frac{x^{\alpha}}{\varepsilon^{\alpha}})$.

Tables 1 - 4 show the numerical errors using the numerical scheme (3.5) with uniform mesh nodes when the small parameter ε are taken as 1.0e-2 - 1.0e-5. These tables show that the numerical scheme with uniform mesh nodes gives a great performance, while it can not achieve a good result since the small parameter ε equals to 1.0e-5, in other words, when the singular perturbation behaves fierce and the inner boundary layer turns very thin.

Table 1. The numerical error, rate and CPU time using regular nodes with ε = 1.0e-2.

N_{uni}	τ	error	order	CPU time
10000	1.0000e-04	2.0254e-03	—-	0.721210
20000	5.0000e-05	1.0282e-03	0.978044	2.100715
40000	2.5000e-05	5.2200e-04	0.978040	9.226536
80000	1.2500e-05	2.6518e-04	0.977051	32.484579

Table 2. The numerical error, rate and CPU time using regular nodes with ε = 1.0e-3.

N_{uni}	τ	error	order	CPU time
10000	1.0000e-04	1.8751e-02	—-	0.812140
20000	5.0000e-05	9.6845e-03	0.953215	2.568955
40000	2.5000e-05	4.9507e-03	0.968036	11.093007
80000	1.2500e-05	2.5189e-03	0.974856	37.120419

Due to the values changing suddenly in the boundary inner layer, we think about increasing the proportion of the number of the boundary inner layer. Then the numerical scheme with Shishkin mesh nodes is applied to solve the example instead. The better performances about approximation accuracy are listed in Tables 5-9 which show the good result even when the small parameter ε is taken as 1.0e-9. At the same time, the CPU time, i.e., the computation is large in these above tables. This motivates us take into further consideration reducing the computation and maintaining the approximation accuracy.

Then the results for the Shishkin scheme (3.5), keeping the number of mesh nodes in boundary inner layer while reducing the one in boundary external layer, are shown

Table 3. The numerical error, rate and CPU time using regular nodes with $\varepsilon = 1.0\text{e-}4$.

N_{uni}	τ	error	order	CPU time
10000	1.0000e-04	1.3514e-00	—-	0.708407
20000	5.0000e-05	7.8415e-02	0.785237	2.135138
40000	2.5000e-05	4.3460e-02	0.851438	9.267519
80000	1.2500e-05	2.3107e-02	0.911372	33.376636

Table 4. The numerical error, rate and CPU time using regular nodes with $\varepsilon = 1.0\text{e-}5$.

N_{uni}	τ	error	order	CPU time
10000	1.0000e-04	9.5725e-02	—-	0.477043
20000	5.0000e-05	1.5671e-00	-0.711150	1.995241
40000	2.5000e-05	1.9257e-00	-0.297277	8.390547
80000	1.2500e-05	1.5661e-00	0.298187	36.994000

Table 5. The numerical error, rate and CPU time using non-regular nodes with $\varepsilon = 1.0\text{e-}5$.

N_{nonuni}	τ_{inner}	τ_{outer}	error	order	CPU time
10000	1.6379e-06	1.1093e-04	2.9608e-02	—-	0.702791
20000	8.8056e-07	5.5458e-05	1.6628e-02	0.929656	2.569509
40000	4.7109e-07	2.7725e-05	9.1447e-03	0.955945	10.890227
80000	2.5095e-07	1.3861e-05	4.9692e-03	0.968430	43.383574

Table 6. The numerical error, rate and CPU time using non-regular nodes with $\varepsilon = 1.0\text{e-}6$.

N_{nonuni}	τ_{inner}	τ_{outer}	error	order	CPU time
10000	1.8377e-07	1.1109e-04	3.2965e-02	—-	0.553446
20000	9.8800e-08	5.5545e-05	1.8537e-02	0.927635	2.134871
40000	5.2858e-08	2.7772e-05	1.0212e-02	0.953168	8.717076
80000	2.8158e-08	1.3886e-05	5.5578e-03	0.965962	53.386006

in Table 10 - Table 14. It can be seen that the computation reduces enormously, simultaneously it maintains the approximation accuracy almost unchanged, which shows good efficiency with Shishkin mesh nodes compared to Table 5 - Table 9 with regular nodes.

Table 7. The numerical error, rate and CPU time using non-regular nodes with $\varepsilon = 1.0\text{e-}7$.

N_{nonuni}	τ_{inner}	τ_{outer}	error	order	CPU time
10000	2.0619e-08	1.1111e-04	3.6562e-02	—	0.782936
20000	1.1086e-08	5.5554e-05	2.0623e-02	0.922662	2.825858
40000	5.9307e-09	2.7777e-05	1.1408e-02	0.946591	10.752474
80000	3.1593e-09	1.3889e-05	6.2146e-03	0.964492	53.722414

Table 8. The numerical error, rate and CPU time using non-regular nodes with $\varepsilon = 1.0\text{e-}8$.

N_{nonuni}	τ_{inner}	τ_{outer}	error	order	CPU time
10000	2.3135e-09	1.1111e-04	4.0386e-02	—	0.649463
20000	1.2438e-09	5.5555e-05	2.3002e-02	0.907006	2.871796
40000	6.6544e-10	2.7778e-05	1.2738e-02	0.944857	11.593306
80000	3.5448e-10	1.3889e-05	6.9482e-03	0.962411	39.322190

Table 9. The numerical error, rate and CPU time using non-regular nodes with $\varepsilon = 1.0\text{e-}9$.

N_{nonuni}	τ_{inner}	τ_{outer}	error	order	CPU time
10000	2.5958e-10	1.1111e-04	4.4981e-02	—	0.554434
20000	1.3956e-10	5.5556e-05	2.5583e-02	0.909300	2.066503
40000	7.4663e-11	2.7778e-05	1.4216e-02	0.939347	11.911500
80000	3.9774e-11	1.3889e-05	7.7668e-03	0.959886	44.398808

Table 10. The numerical error, rate and CPU time using less non-regular nodes with $\varepsilon = 1.0\text{e-}5$.

N_{nonuni}	τ_{inner}	τ_{outer}	error	order	CPU time
800	2.2228e-06	1.3886e-03	3.8945e-02	—	0.025761
1600	1.1114e-06	6.9432e-04	2.0675e-02	0.913533	0.025532
3200	5.5571e-07	3.4716e-04	1.0720e-02	0.947669	0.091094
6400	2.7786e-07	1.7358e-04	5.4863e-03	0.966338	0.281511

4.2. An example with variable coefficient

In this section we study the problem with variable coefficient:

$$\begin{cases} \varepsilon^{\alpha}\,{}_{0}^{\mathrm{C}}D_x^{\alpha}u(x) + (1/2 + x\sin x + e^x)u(x) = f(x), \quad x \in (0,1], \\ u(0) = 1, \end{cases}$$

Table 11. The numerical error, rate and CPU time using less non-regular nodes with ε = 1.0e-6.

N_{nonuni}	τ_{inner}	τ_{outer}	error	order	CPU time
800	2.4941e-07	1.3889e-03	4.3365e-02	—	0.004216
1600	1.2470e-07	6.9443e-04	2.3057e-02	0.911334	0.002885
3200	6.2352e-08	3.4722e-04	1.1969e-02	0.945908	0.067662
6400	3.1176e-08	1.7361e-04	6.1352e-03	0.964119	0.261528

Table 12. The numerical error, rate and CPU time using less non-regular nodes with ε = 1.0e-7.

N_{nonuni}	τ_{inner}	τ_{outer}	error	order	CPU time
800	2.7984e-08	1.3889e-03	4.8057e-02	—	0.009035
1600	1.3992e-08	6.9444e-04	2.5647e-02	0.905997	0.002725
3200	6.9960e-09	3.4722e-04	1.3359e-02	0.940906	0.061072
6400	3.4980e-09	1.7361e-04	6.8594e-03	0.961711	0.203149

Table 13. The numerical error, rate and CPU time using less non-regular nodes with ε = 1.0e-8.

N_{nonuni}	τ_{inner}	τ_{outer}	error	order	CPU time
800	3.1399e-09	1.3889e-03	5.2810e-02	—	0.021829
1600	1.5699e-09	6.9444e-04	2.8527e-02	0.888495	0.021615
3200	7.8496e-10	3.4722e-04	1.4908e-02	0.936208	0.057694
6400	3.9248e-10	1.7361e-04	7.6669e-03	0.959385	0.200649

Table 14. The numerical error, rate and CPU time using less non-regular nodes with ε = 1.0e-9.

N_{nonuni}	τ_{inner}	τ_{outer}	error	order	CPU time
800	3.5230e-10	1.3889e-03	5.8116e-02	—	0.020971
1600	1.7615e-10	6.9444e-04	3.1671e-02	0.875765	0.004222
3200	8.8074e-11	3.4722e-04	1.6632e-02	0.929239	0.092106
6400	4.4037e-11	1.7361e-04	8.5684e-03	0.956843	0.200532

where $\alpha = 0.8$, $f(x) = \Gamma(\alpha+1)\varepsilon^\alpha + (1/2 + x\sin x + e^x)E_\alpha(-\frac{x^\alpha}{2\varepsilon^\alpha})$ and exact solution $u(x) = x^\alpha + E_\alpha(-\frac{x^\alpha}{2\varepsilon^\alpha})$.

Figures 1 and 2 show the exact solutions' behavior which reflects the existence of the boundary layer when the small parameters ε are taken from 1.0e-1 to 1.0e-8. Along with ε becoming smaller, the boundary layer of the solution becomes narrow rapidly.

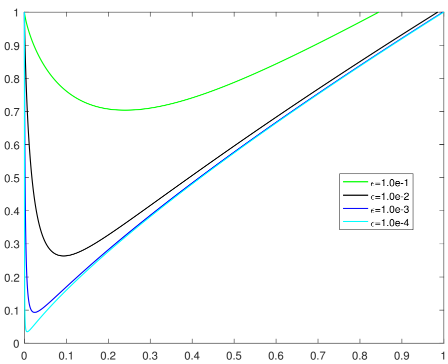

Figure 1. Exact solutions for ε = 1.0e-1 $\sim$ 1.0e-4.

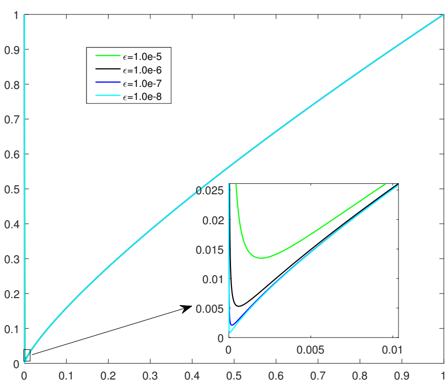

Figure 2. Exact solutions for ε = 1.0e-5 $\sim$ 1.0e-8.

To reduce the computation, we take Shishkin nodes' number as only taken twenty percent of exact solution' node number. The numerical solutions are shown in Figures 3 - 6 as the small parameter ε is taken as = 1.0e-5 $\sim$ 1.0e-8. The smaller figures in the Figures 3 - 6 show the good approximation along with ε becomes smaller.

4.3. An example with spatial Riemann-Liouville fractional derivative

In this section we consider the application of the Shishkin mesh scheme in the partial differential equation:

$$\begin{cases} \varepsilon^{\alpha}\,{}_0^{\mathrm{C}}D_t^{\alpha}u(x,t)+u(x,t)={}_0^{\mathrm{R}}D_x^{\beta}u(x,t)+f(x,t), \quad (x,t)\in[0,1]\times(0,1], \\ u(x,0)=x^2-x^3,\ \ x\in[0,1], \\ u(0,t)=u(1,t)=0,\ \ t\in(0,1], \end{cases}$$

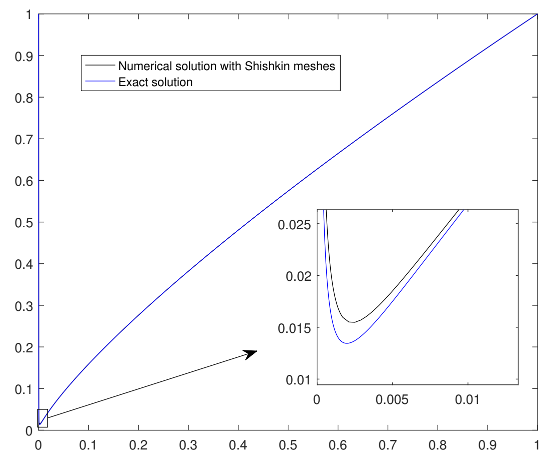

Figure 3. Numerical solution with Shishkin meshes and exact solution for ε = 1.0e-5.

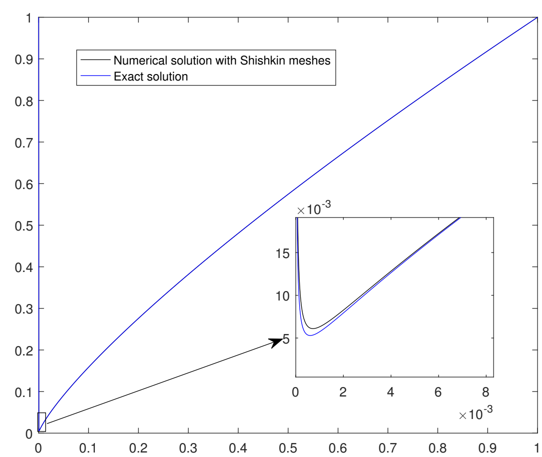

Figure 4. Numerical solution with Shishkin meshes and exact solution for ε = 1.0e-6.

where $\alpha = 0.9,\ \beta = 1.8,\ f(x) = -E_\alpha(-\frac{t^\alpha}{\varepsilon^\alpha})(\frac{\Gamma(3)}{\Gamma(3-\beta)}x^{2-\beta} - \frac{\Gamma(4)}{\Gamma(4-\beta)}x^{3-\beta})$ and exact solution $u(x) = E_\alpha(-\frac{t^\alpha}{\varepsilon^\alpha})(x^2 - x^3)$. And the symbol ${}_0^{\mathrm{R}}D_x^\beta$ means Riemann-Liouville fractional derivative as defined by:

$$ {}_0^{\mathrm{R}}D_x^\beta v(x) = \frac{1}{\Gamma(2-\beta)}\frac{d^2}{dx^2}\int_0^x \frac{v(\xi)}{(x-\xi)^{\beta-1}}d\xi, $$

which can be discretized as [10]:

$$ {}_0^{\mathrm{R}}D_x^\beta v(x_i) \approx \frac{1}{h_x^\beta \Gamma(2-\beta)}\sum_{j=0}^{i} g_{\beta,j}v(x_{i-j+1}), $$

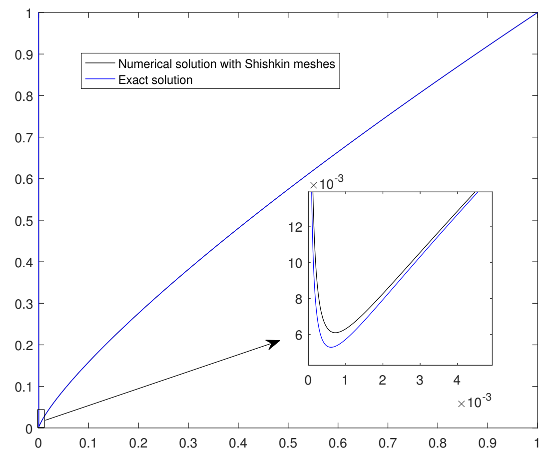

Figure 5. Numerical solution with Shishkin meshes and exact solution for $\varepsilon = 1.0\text{e-}7$.

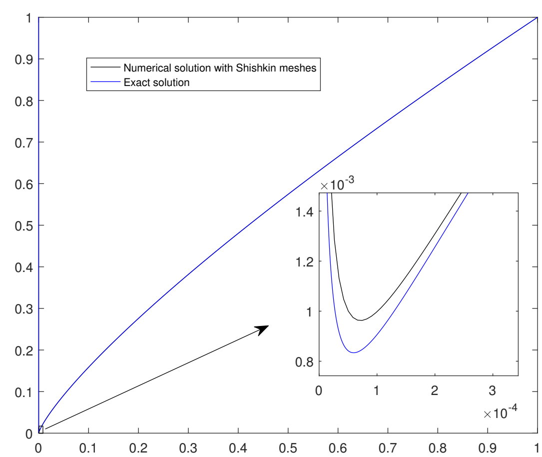

Figure 6. Numerical solution with Shishkin meshes and exact solution for $\varepsilon = 1.0\text{e-}8$.

where the weight $g_{\beta,j}$ is denoted as

$$g_{\beta,j} = \frac{\Gamma(j-\beta)}{\Gamma(-\beta)\Gamma(j+1)}.$$

The numerical solutions, with Shishkin mesh nodes in temporal direction and regular nodes in spatial direction, are shown in Figures 7-10 as the small parameters ε are taken as $= 1.0\text{e-}5 \sim 1.0\text{e-}8$. And the solution for $x = 0.125$ at $t = 0.001$ when $\varepsilon = 1.0\text{e-}5, 1.0\text{e-}8$ are shown in Figures 11 and 12, which testifies good efficiency applied in partial fractional differential equation with small parameter.

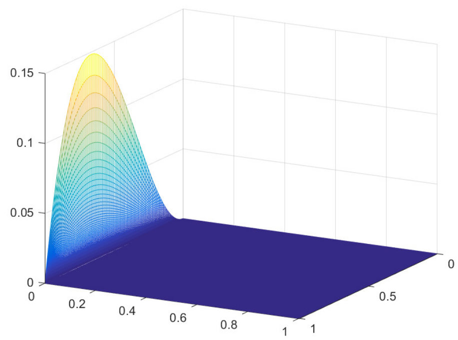

Figure 7. Numerical solution with Shishkin mesh nodes for ε = 1.0e-5.

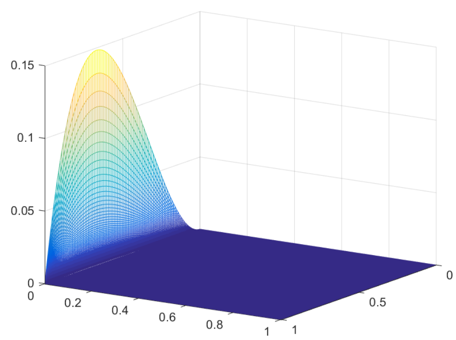

Figure 8. Exact solution for ε = 1.0e-5.

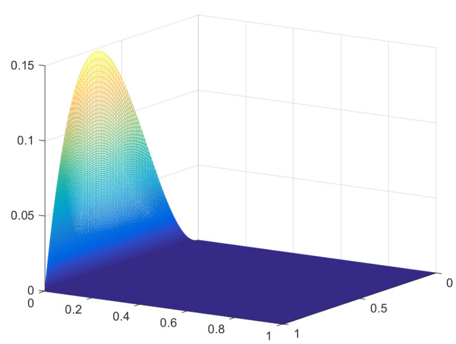

Figure 9. Numerical solution with Shishkin mesh nodes for ε = 1.0e-8.

5. Conclusion

In this paper, we considered the singular perturbation Cauchy problem with small parameter as the coefficient of the fractional order derivative term. We dealt with the property of the solution for the singular perturbation problem and deduced its

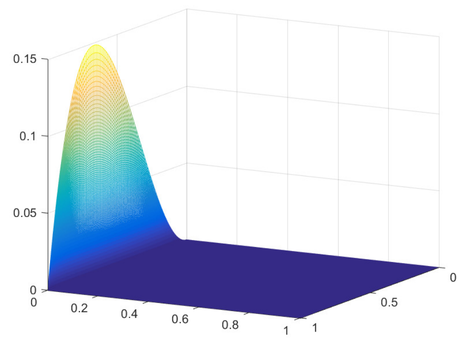

Figure 10. Exact solution for $\varepsilon = 1.0\text{e-}8$.

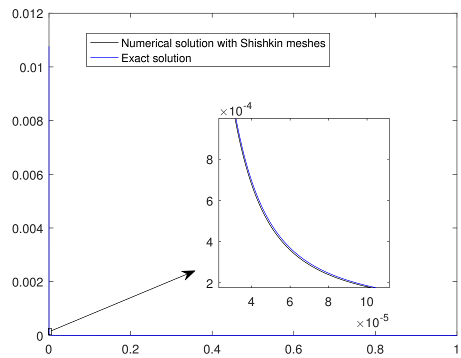

Figure 11. Numerical solution with Shishkin meshes for $x = 0.125$ at $t = 0.001$ for $\varepsilon = 1.0\text{e-}5$.

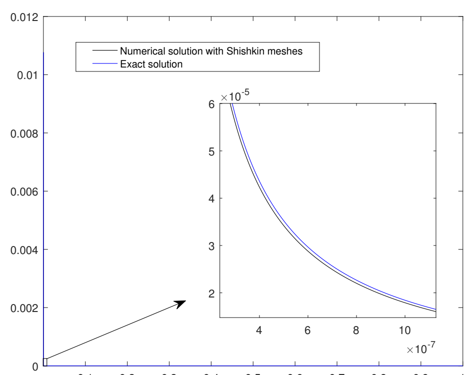

Figure 12. Numerical solution with Shishkin meshes for $x = 0.125$ at $t = 0.001$ for $\varepsilon = 1.0\text{e-}8$.

stability by Maximum theorem. Furthermore, we proposed the numerical simulation with regular meshes and Shishkin meshes. Finally, numerical examples in one-dimension and two-dimension case were testified to exhibit the effects.

References

[1] E. Alvarez and C. Lizama, *The super-diffusive singular perturbation problem*, Mathematics, 2020, 8, 403, 1–14. DOI: 10.3390/math8030403.

[2] B. Asarel, M. Sah and R. K. Hona, *Alternative methods of regular and singular perturbation problems*, Applied Mathematics, 2024, 15(10), 687–708.

[3] X. Cai and F. W. Liu, *Uniform convergence difference schemes for singularly perturbed mixed boundary problems*, Journal of Computational and Applied Mathematics, 2004, 166, 31–54.

[4] D. Chaikoskii and N. Mingkand, *Internal layers for a singularly perturbed differential equation with Robin boundary value condition*, Journal of East China Normal University (Natural Science), 2020, 2, 23–34.

[5] V. Georgiev and M. Rastrelli, *Sobolev spaces for singular perturbation of 2D Laplace operator*, Nonlinear Anal. TMA, 2025, 251, 113710.

[6] R. Gorenflo and F. Mainardi, *Fractional calculus: Integral and differential equations of fractional order*, cited as arXiv: 0805.3823, and published on the page 223–276 of the book: A. Carpinteri and F. Mainardi (Editors): Fractals and Fractional Calculus in Continuum Mechanics, Springer Verlag, Wien and New York, 1997. DOI: 10.1007/978-3-7091-2664-6_5.

[7] X. L. Han, L. F. Shi, Y. H. Xu and J. Q. Mo, *Asymptotic solution for the fractional order singularly perturbed nonlinear differential equation with two parameters*, Acta Mathematicae Applicatae Sinica, 2015, 38(4), 721–729.

[8] K. Kumar, P. Chakravarthy and V. Aguiar, *Numerical solution of time-fractional singularly perturbed convection–diffusion problems with a delay in time*, Math Meth Appl Sci. Special Issue Paper, 2020, 1–18.

[9] X. Y. Lin and F. Xie, *Singular perturbation for a kind of nonlinear fractional differential equations*, Journal of Donghua University, 2009, 35(2), 238–240.

[10] Q. X. Liu, F. W. Liu, I. Turner and V. Anh, *Numerical simulation for the 3D seepage flow with fractional derivatives in porous media*, IMA Journal of Applied Mathematics, 2009, 74, 201–229.

[11] Y. Luchko, *Maximum principle for the generalized time-fractional diffusion equation*, Journal of Mathematical Analysis and Applications, 2009, 351, 218–223.

[12] M. Mariappan, *An efficient computational algorithm for a class of nonlinear singular perturbation problems of convection diffusion type with Cauchy data*, Journal of Nonlinear Science, 2025, 35(1), 1–19.

[13] J. J. H. Miller, E. O'Riordan and G. I. Shishkin, *Fitted Numerical Methods for Singular perturbation Problems: Error Estimates in the Maximum Norm for Linear Problems in One and Two Dimensions*, Singapore: World Scientific, 1996.

[14] I. Podlubny, *Fractional Differential Equations, Academic Press*, San Diego, California, 1999.

[15] M. Rezapour, *The Caputo-Fabrizio fractional derivative applied to a singular perturbation problem*, International Journal of Mathematical Modelling and Numerical Optimisation, 2020, 9(3), 241–253.

[16] Z. Sabir and M. R. Ali, *Analysis of perturbation factors and fractional order derivatives for the novel singular model using the fractional Meyer wavelet neural networks*, Chaos, Solitons and Fractals: X, 2023, 11, 100100.

[17] D. Y. Shi and Y. M. Wu, *Uniformly superconvergent analysis of an efficient two-grid method for nonlinear Bi-wave singular perturbation problem*, Applied Mathematics and Computation, 2020, 367, 124772.

[18] L. F. Shi and J. Q. Mo, *Asymptotic solution for a class of semilinear singularly perturbed fractional differential equation*, Chinese Physics B, 2010, 19(5), 050203.

[19] G. I. Shishkin, *Discrete Approximation of Singularly Perturbed Elliptic and Parabolic Equation (Russian), Second Doctorial Thesis*, Keldysh Institure, Moscow, 1990.

[20] E. R. El-Zahar, G. F. Al-Boqami and H. S. Al-Juaydi, *Piecewise approximate analytical solutions of high-order reaction-diffusion singular perturbation problems with boundary and interior layers*, AIMS Mathematics, 2024, 9(6), 2024756.

[21] Y. N. Zhang, Z. Z. Sun and H. L. Liao, *Finite difference methods for the time fractional diffusion equation on non-uniform meshes*, Journal of Computational Physics, 2014, 265, 195–210.

[22] H. B. Zhu, *Singular perturbation boundary value problem for a fractional differential equation of order* 2α, Journal of Anhui University of Technology (Natural Science), 2018, 35(1), 85–89.

Received January 2025; Accepted April 2025; Available online May 2025.